Engineering Conferences International
ECI Digital Archives

10th International Conference on Circulating Fluidized Beds and Fluidization Technology - CFB-10

Refereed Proceedings

Spring 5-4-2011

Study of Standpipe and Loop Seal Behavior in a Circulating Fluidized Bed for Geldart B Particles

Heiko Dieter
Institute of Combustion and Power Plan Technology, University of Stuttgart

Alexander Charitos
Institute of Combustion and Power Plan Technology, University of Stuttgart

Ajay R. Bidwe
Institute of Combustion and Power Plant Technology (IFK), University of Stuttgart

An Wei
Institute of Combustion and Power Plant Technology (IFK), University of Stuttgart

Mariusz Zieba
Institute of Combustion and Power Plant Technology (IFK), University of Stuttgart

A STUDY OF STANDPIPE AND LOOP SEAL BEHAVIOR IN A CIRCULATING FLUIDIZED BED FOR GELDART B PARTICLES

Ajay R. Bidwe, Alexander Charitos, Heiko Dieter, An Wei, Mariusz Zieba,
Günter Scheffknecht
Institute of Combustion and Power Plant Technology (IFK), University of Stuttgart,
Pfaffenwaldring 23, 70569, Stuttgart, Germany.
Email: bidwe@ifk.uni-stuttgart.de

ABSTRACT

The loop seal aeration effect on the supply side has been studied through small scale CFB experimentation. Parameters affected include inventory allocation and entrainment. The gas velocity in the standpipe is influenced by loop seal aeration and riser velocity. Variation in slugging behavior above and below solid downflow velocity of 0.025 m/s is analyzed and discussed here.

INTRODUCTION

Circulating fluidized bed (CFB) technology is used in various applications including combustion of solid fuels for electricity production (1). Recently, it has been applied in the field of solid looping cycles aiming at CO_2 capture, such as calcium looping (2), and chemical looping combustion (3). For combustors standalone CFB's are used, while for solid looping cycles dual fluidized bed (DFB) systems are utilized. In both cases the standpipe-loop seal arrangement is an important component. A typical standalone CFB consists of a riser, cyclone and standpipe-loop seal arrangement, shown in Fig. 1. The loop seal acts as a solid pumping device from the low pressure cyclone to the high pressure riser and ensures that riser gas does not take the short cut through the cyclone. In comparison, DFB systems consist commonly of two CFBs or a CFB and a BFB, depending on the facility purpose (2). In this case the role of a loop seal is to transfer solids from the low pressure cyclone of one reactor to a high or low pressure point of the other reactor, while disallowing gases from one reactor to enter the other. In both cases, standpipe-loop seal operation is indispensible. Solid downflow, within the standpipe and loop seal occurs in three modes as explained by Knowlton (4). Moving bed mode, bubbling fluidized mode are possible below the level of the particle bed, L_{st}. Above this level solid flow occurs in dilute mode. A bubbling or moving bed

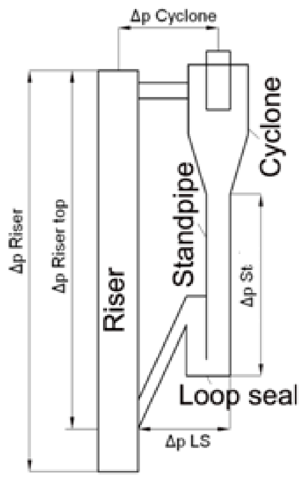

Figure 1- Stand alone CFB

standpipe is common in CFB applications and is considered to be stable. However, in small scale facilities, slugging may occur as a result of small scale standpipe diameter and is threatening to operational stability. The loop seal itself consists of two sections, the supply section and the recycle section, as shown in Fig. 2. The supply section is fed with a particle flow from the riser cyclone. This flow proceeds through the slit and the recycle section back to the riser or, in the case of DFB systems, to the other reactor.

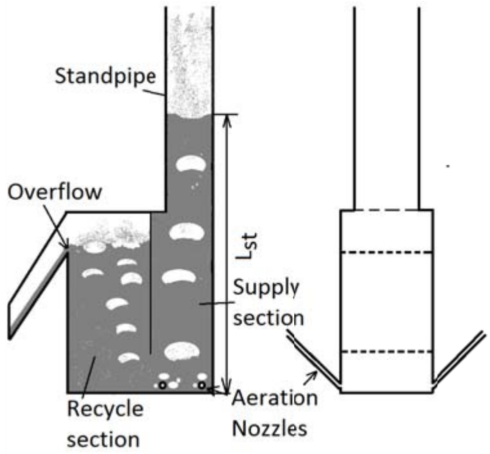

Figure 2- Standpipe and loop seal

For above mentioned DFB processes the loop seal is an important part but gases used in loop seal aeration could be a source of dilution for product gases. Therefore optimizing the loop seal design is important for these processes. Considerations for standpipe, loop seal design and operation, to which this paper aims to contribute to, are summarized below: (i) the loop seal aeration effect on solid inventory, riser entrainment (ii) the split of this aeration flow between the loop seal supply and recycle chamber (iii) hydrodynamic stability through avoidance of slugging operation in the standpipe. In normal loop seal operation both sections of the loop seal are fluidized. However to investigate the aeration split systematically it was decided to aerate only in the supply section. By doing this the effect of loop seal aeration only in the supply section can also be investigated.

TEST FACILITY AND EXPERIMENTAL PROCEDURE

The test facility consists of a CFB system, as shown in Fig. 1 and is constructed from transparent plexi-glass. The dimensions of the CFB are shown in Table 1. The aeration nozzles, located only in the supply section of the loop seal are inserted sideways at an angle of 45°, to prevent particles clogging the gas nozzles. The fluidization gas is air and particles are Ilmenite mineral particles with a particle size distribution of 100-200 µm and a mean particle size of 143 µm. The particle density (ρ_s) is 4400 kg/m³ and the Geldart classification of particles is class B (5). The u_{mf} is calculated, as shown in (1), to be equal 0.029 m/s. Pressure transducers are mounted at various locations of the CFB system. Rotameters are used to measure the air supply to the riser and loop seal. The facility is filled with a known total solid inventory (TSI). The parameters varied are the loop seal aeration (u_{LS}) in wide range of 0.003 to 0.28 m/s and riser velocity 3 to 5 m/s. The entrainment is measured through stopping loop seal aeration and measuring the accumulation of the particle bed height with the standpipe for a given period of time.

Table 1 :Dimensions of CFB

Riser		
Riser diameter	[mm]	70
Riser height	[m]	4
Standpipe H / Dia	[m]	1/0.03
Loop seal		
Height	[mm]	200
Supply Length	[mm]	35
Recycle Length	[mm]	50
Width	[mm]	35
Weir height	[mm]	150
Slit opening	[mm]	30

Loop seal aeration flow path determination

The data evaluation procedure is based on Basu & Cheng (7) and has been applied for every steady state. Goal of the analysis, presented in steps, is to define the gas flow path through the loop seal.

(i) Calculation of the standpipe slip velocity

The slip velocity (U_{sl}), expresses the relative velocity between gas and solid within

$$\Delta p_{St} = \left(\frac{\Delta p}{dz}\right)_{St} L_{St} = \left(\frac{150\mu(1-\varepsilon)^2}{(\varphi d_p)^2 \varepsilon^2}|U_{sl}| + \frac{1.75\rho_g(1-\varepsilon)}{(\varphi d_p)\varepsilon}|U_{sl}|^2\right) L_{St} \quad (1)$$

the standpipe and is calculated through Eq.1. The pressure drop through the standpipe (Δp_{St}) and the particle bed height (L_{St}) have been measured for every steady state, thus defining also the pressure gradient $\left(\frac{\Delta p}{dz}\right)_{St}$.The Δp_{St} is measured from the bottom of the loop seal to the bottom of the cyclone. Althought the areas of standpipe and loop seal vary, but for simplification the $\left(\frac{\Delta p}{dz}\right)_{St}$ is assumed to be constant and further calculations of gas and solid velocity are based on the area of standpipe. The voidage (ε) value, for packed bed column found to be equal to 0.48 and at minimum fluidizing conditions (ε_{mf}) is found to be 0.54. However the exact voidage while standpipe operation is difficult to estimate. Therefore an average voidage of 0.51 is considered for calculation. Eq.1 has been applied only when the fluidization regime in the standpipe was moving bed. The situations in which this standpipe showed bubbling or slugging mode of fluidization are not considered in the calculations. The sphericity of the particles (φ) has been taken as 0.75 from voidage-sphericity graphs in (6).

(ii) Calculation of the real solid downflow and gas velocity

The real solid downflow velocity (U_s) and gas velocity (U_g) is calculated through Eq. (2) and Eq. (3). The U_s and U_g are positive in the downwards direction. The $G_{s\,St}$ is defined through measurement of the riser entrainment, based on the standpipe cross-section (A_{St}). The real standpipe gas velocity (U_g) is subsequently calculated through Eq. 3, which is the definition of the slip velocity. The superficial gas velocity (u_g) in the standpipe is calculated from the voidage.

$$U_s = \frac{G_{s\,St}}{\rho_s(1-\varepsilon)} \quad (2) \qquad U_{sl} = U_s + U_g \quad (3)$$

(iii) Calculation of loop seal aeration split

The flow travelling through the particle column in the standpipe (U_g) is given by Eq.4. If $(\dot{V}_S)$ is positive than the loop seal aeration flow is split between the loop seal supply chamber-standpipe and the recycle chamber-riser. This split is quantified with the ratio of Eq.5 and is defined as the fraction of total volumetric flow of the loop seal aeration $(\dot{V}_T)$ entering supply side $(\dot{V}_S)$ or the recycle side $(\dot{V}_R)$ of the loop seal. The aeration split in the supply section is calculated using Eq.5 and the recycle side given by Eq.6. If the $\dot{V}_s$ is negative, the gas flow from the cyclone is carried downwards with the particles. This carried gas from the particles enters the recycle chamber ($\dot{V}_R$) in addition to the loop seal aeration ($\dot{V}_T$).

$$\dot{V}_s = U_g \varepsilon A_{St} = u_g A_{St} \quad (4) \qquad Aeration\ split\ (supply) = \frac{\dot{V}_s}{\dot{V}_T} \quad (5)$$

$$Aeration\ split\ (recycle) = \frac{\dot{V}_R}{\dot{V}_T} = 1 - \left(\frac{\dot{V}_s}{\dot{V}_T}\right) \quad (6)$$

Pressure balance

The pressure balance for the system of Fig.1 is given by Eq.7 (7) (9).

$$\Delta p_{St} = \Delta p_{LS} + \Delta p_{Riser\ top} + \Delta p_{Cyclone} \quad (7)$$

The pressure drop terms of Eq.7 are depicted in Fig.1.

RESULTS AND DISCUSSION

The effect of the loop seal aeration in the supply section is examined, with respect to the parameters below.

Riser pressure drop

Fig.3 shows the effect of the loop seal aeration on the riser pressure drop. The loop seal becomes functional when $\frac{u_{LS}}{u_{mf}} > 2$. Its velocity ($u_{LS}$) is calculated based on the total area of the loop seal including supply and recycle chamber given in Table 1. Increasing loop seal aeration decreases the standpipe particle bed height (L_{St}) and increases its pressure drop (Δp_{St}). This is explainable due to the increase of $\left(\frac{\Delta p}{dz}\right)_{St}$, as expected from Eq.1. For constant riser superficial velocity, the increase of loop seal aeration causes an increase in riser pressure drop (Δp_{Riser}). This is a result of mass transfer from the standpipe, noticed as a decrease of standpipe height (L_{St}), to the riser. A similar observation is reported by Charitos et al (2). However, most of the riser inventory is located in the bottom part therefore slope of increase of Δp_{Riser} is bigger than that of the standpipe pressure drop (Δp_{St}), this follows the pressure balance as per Eq.7.

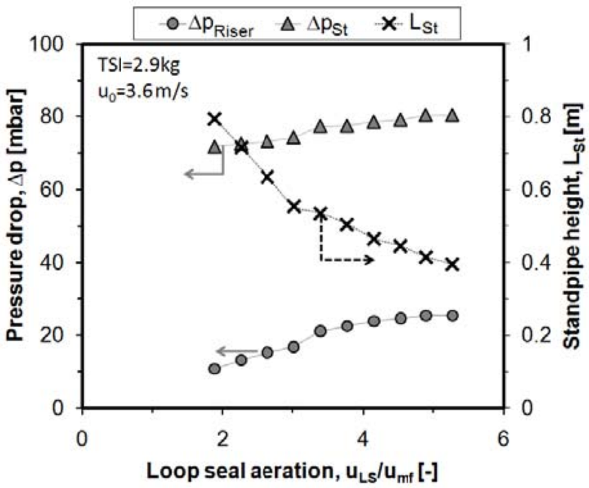

Figure 3- Effect of loop seal aeration on standpipe height, pressure drop and riser pressure drop

Riser entrainment The riser entrainment (G_s) is plotted against the loop seal aeration ratio $\left(\frac{u_{LS}}{u_{mf}}\right)$ in Fig.4. For both riser velocities realized during experiments, increasing loop seal aeration results in an increase of G_s until a maximum is reached ([5])([7])([8]). This can be explained since increasing loop seal aeration results in an increase of Δp_{Riser} as shown in Fig. 3. For a riser velocity (u_0) of 3.6 m/s the G_s maximum is equal to 23.5 kg/m^{2}s at a loop seal aeration ratio $\frac{u_{LS}}{u_{mf}}$ of 3.6. For the higher u_0 of 4.3 m/s the maximum G_s is equal to 28.7 kg/m^{2}s occurring at $\frac{u_{LS}}{u_{mf}}$ of 6.6. Further aeration reduces the G_s slightly. A number of works, e.g. ([7]) and ([9]), do not predict a reduction of G_s with loop seal aeration. However, Lee et al. ([10]) has reported such behavior in a seal pot for Geldart A particles. In this work the decrease of G_s beyond its maximum coincides and may be attributed to the appearance of the slugging in the standpipe. Finally, for a given $\frac{u_{LS}}{u_{mf}}$ value, increasing riser velocity u_0 results in a higher G_s value, as reported in many works, e.g. ([2]).

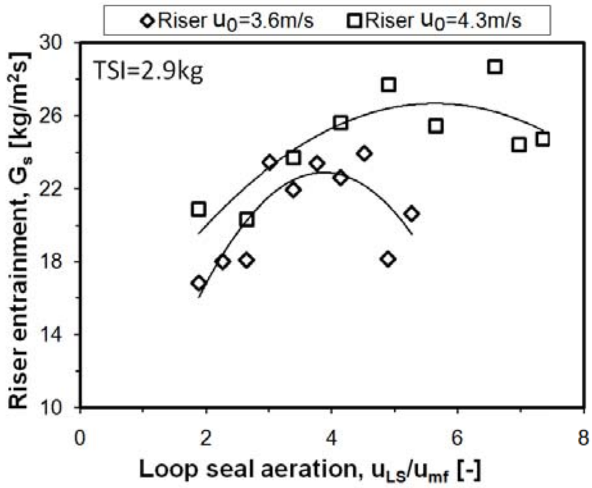

Figure 4- Effect of loop seal aeration on riser entrainment G_s at two velocities. TSI -2.9 kg.

Gas velocity through the standpipe

Fig.5 and Fig.6 depict the effect of the loop seal aeration ratio ($\frac{u_{LS}}{u_{mf}}$) on the superficial gas velocity in the standpipe (u_g) and the aeration split respectively defined in Eq.5, at riser velocity of 3.6 and 4.3 m/s. The superficial gas velocity is calculated as a product of the real gas velocity (U_g) and the voidage (ε) shown in Eq.4. The voidage considered for calculation is 0.51. As seen in Fig.5 an increase of $\frac{u_{LS}}{u_{mf}}$ results in an increase of u_g for the riser velocity (u_0) of 3.6 m/s almost linearly. For higher riser velocity of 4.3 m/s and loop seal aeration ratios $\frac{u_{LS}}{u_{mf}}$<5.6, u_g is in the range of -0.02 m/s. The gas flow in the standpipe is moving downwards, when u_g and the aeration split values are negative. For the lower u_0 of 3.6 m/s, this phenomenon is encountered for a smaller $\frac{u_{LS}}{u_{mf}}$ range, namely when $\frac{u_{LS}}{u_{mf}}$ < 2.6. For a given $\frac{u_{LS}}{u_{mf}}$ value, the u_g is higher at a u_0 of 3.6 m/s in comparison to a u_0 of 4.3 m/s. These observations can be explained based on the higher G_s values, resulting in higher U_s values (see Eq.3), occurring at a u_0 of 4.3 m/s in comparison to a u_0 3.6 m/s, as shown in Fig. 4. This is based on that higher G_s. Higher U_s values result in a higher resistance for gas up flow in the standpipe. However, when the $\frac{u_{LS}}{u_{mf}}$ ratio is increased enough, then the u_g and aeration split become positive, thus indicating that the gas flow in the standpipe is upwards. It can be observed that the downward u_g have a limitation, i.e. -0.03 m/s. Basu and Butler([8]) have the similar conclusion.

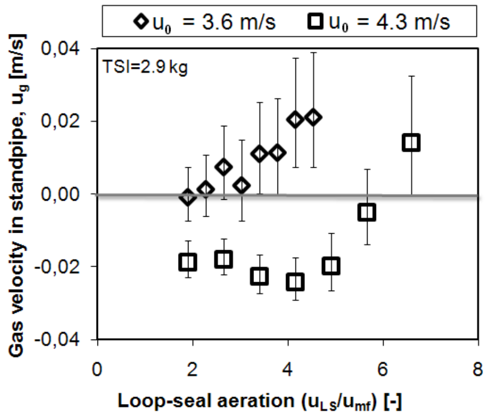

Figure 5 – Effect of loop seal aeration on gas velocity in standpipe (u_g) at different riser velocities u_0 (TSI =2.9 kg)

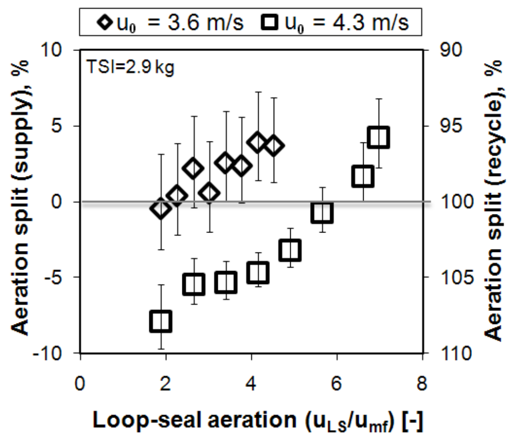

Figure 6 – Effect of loop seal aeration on the aeration split

The aeration split increases with increase in $\frac{u_{LS}}{u_{mf}}$ and is calculated from -8% to +6%. Up to 6% of the aeration gas is entering the standpipe. This concludes that remaining 94-100% of the aeration gas is entering the recycle chamber. In case of negative u_g additional gas is entering the recycle side of the loop seal. If the calculated aeration in the recycle side is in the range of 2-6 u_{mf} and enough to keep the recycle side of the loop seal fluidized. Therefore the loop seal worked well even without the aeration in the recycle chamber.

The deviation bars in Fig.5 and Fig.6 show the influence of voidage in the calculations of u_g and aeration split. The lower deviation shows the value at a voidage of 0.48 and the upper deviation shows the value of voidage 0.54 close to u_{mf}. As observed the voidage can affect the results significantly. As discussed earlier, the assumption of a constant $\left(\frac{\Delta p}{dz}\right)_{St}$, despite the two different standpipe cross-sections, holds true to a limited extent. Therefore, to find out the exact gas flow pattern would implicate the use of tracer gases. Johansson et al (3) reported aeration split values of 2 to 7 % using tracer gases. In that work, for a separate downcomer of the same facility U_g values of -0.05 m/s to + 0.1 m/s were recorded. Hence the results reported in this section are comparable with the data of (3).

Slugging in the standpipe

Fig.5 and Fig.6 show that the increasing loop seal aeration increases the gas velocity in the standpipe. At low or negative gas velocities the standpipe was in moving bed mode. With increasing aeration in the loop seal a stage is reached when bubbles start to appear in the standpipe. The bubbles could be equivalent to a standpipe diameter in such small standpipe used in this study. This situation is commonly referred as slugging, common phenomenon for such small scale units. Two types of slugging have been described by Wen (5). Type A- Round nose slugging and Type B - Flat nose slugging. The Type A is similar to normal bubbling bed where bubbles rise up in fluidized bed. The difference compared to bubbling bed is that a gas slug is nearly equal to the standpipe diameter. Typical Type B slugging is shown in Fig.7 where gas slug completely occupies the cross section and lift the solid chunk above it. The solid downward motion is only possible by raining down as solid streamers or when the chunk gets broken. The Type B slugging occurs mainly with cohesive particles and is not a suitable mode for the standpipe to operate because sometimes the chunks may be lifted up to the cyclone and cause frequent operational break downs.

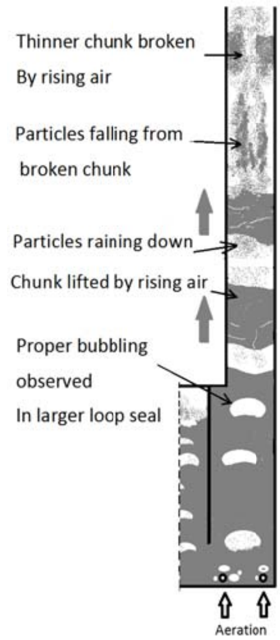

Figure 7- Slugging in standpipe

Such Type B slugging occurred during the experiments at riser velocities of 3.6 and 4.3 m/s and has caused reduction in the entrainment rate (see Fig.4). Typically Type B slugging occurred at U_s > 0.03 m/s while Type A or bubbling occurred at U_s < 0.025. Sometimes both types occurred simultaneously, i.e. Type B in the standpipe and Type A in the loop seal supply side where cross section is larger than standpipe. This clearly shows the influence of solid velocity on the Type of slugging. This fact can be explained as follows: Increasing loop seal aeration increases the gas velocity in the standpipe and at lower solid velocity (U_s<0.025 m/s), the particles bed is expandable and allows smooth bubble travel. At higher solid velocities (U_s>0.03 m/s) the particles tend to flow closely packed, at the same time increasing gas velocity in the standpipe tries to expand the bed. This counter acting behavior of gas and solid leads to the Type B slugging depicted in Fig.7. Since Type B is common to cohesive particles, thus at higher down flow solid velocity the particles exhibit cohesive nature.

In certain applications like calcium looping (2), the preferred fluidization mode in standpipe is bubbling to prevent the calcium particles from sticking together (1). For large scale facilities such slugging may not be relevent. However in small facilities, for certain conditions Type A slugging is unavoidable. The above results give suggestions how to prevent the standpipe from operating in the Type B slugging mode. To avoid Type B slugging it is suggested that U_s in the standpipe is kept lower than 0.025 m/s. Which can be achieved either by reducing the riser entrainment or by increasing the standpipe area A_{st}.

CONCLUSIONS

The standpipe-loop seal behavior in small scale CFB is studied through variation of the loop seal aeration of the supply chamber using Ilmenite particles. The standpipe gas velocity and aeration split in the standpipe increases with increasing loop seal aeration. Increasing the downflow solid velocity decreases the gas velocity and aeration split for a given loop seal aeration. An increment in the loop seal aeration increases the riser G_s up to a limit and then decreases due to slugging in the standpipe. The standpipe slugged easily due to its small diameter. However at solid velocities up to 0.025 m/s Round nose slugging occurred while at higher solid velocity i.e. above 0.03 m/s Flat nose slugging occurred. For a stable CFB operation Flat nose slugging should be avoided.

ACKNOWLEDGEMENTS

This work is part of the ongoing CAL-MOD Project which is funded in part by the RFCS Research Program of the European Commission (RFCR-CT-2010-00013).

NOTATIONS

A_{st}	m²	Standpipe area	U_g	m/s	Real gas velocity in the standpipe
d_p	m	Particle diameter	u_{LS}	m/s	Gas velocity in loop seal
G_s	kg/m^{2}s	riser circulation rate	U_{sl}	m/s	Slip velocity
Δp_i	mbar, Pa	Pressure drop in a given CFB section i	U_s	m/s	Real solid velocity in the standpipe
u_0	m/s	Riser superficial velocity	u_{mf}	m/s	Minimum fluidization velocity
u_g	m/s	Superficial gas velocity in standpipe	$\dot{V}$	m³/s,	Volumetric flow rate

Greek symbols

ε		Voidage	ρ_q	kg/m³	Gas density
μ	Pa.s	Gas viscosity	ρ_s	kg/m³	Particle density
φ		Sphericity			

Abbreviations

CFB	Circulating fluidized bed	St	Standpipe
DFB	Dual fluidized bed	TSI	Total solid inventory
LS	Loop seal		

REFERENCES

1. Basu P., (2006)"Combustion and Gasification in fluidized beds".*Taylor & Francis Group*.
2. Charitos A. Hawthorne C., Bidwe A.R., Korovesis L., Schuster A. and Scheffknecht G. (2010), "Hydrodynamic analysis of a 10 kWth Calcium Looping Dual Fluidized Bed for post-combustion CO_2 capture", *Powder technology*, 200(3), 117–127.
3. Johansson E., Lyngfelt A., Mattisson T. and Johnsson F. (2003), "Gas leakage measurements in a cold model of an interconnected bed for chemical looping combustion." *Powder Technology*, 134(3), 210-217.
4. Knowlton T.M. Handbook of fluidization and fluid particle systems, Chapter 21, Standpipes and Nonmechanical valves. *Taylor and Francis group LLC*.
5. Wen-Ching Yang. Handbook of fluidization and fluid particle systems, Chapter 3, Bubbling fluidized beds, *Taylor and Francis group LLC*
6. Kunni D. and Levenspiel O.,(1991), Fluidization engineering, *A Butterworth-Heinemann*
7. Basu P. and Cheng L., (2000), "An analysis of loop seal operations in a circulating fluidized bed.", *Chemical Engineering Research and Design,* 78(7), 991-998.
8. Basu P. and Butler J., (2009),"Studies on the operation of loop seal in ciruculating fludized bed boilers.", *Applied energy*, 86(9),1723-1731.
9. Kim S.W., Namkung W. and Kim S.D. (1999), "Solid flow characteristics in loop seal of circulating fludized bed.", *Korean J. of chemical eng.,* 16(1), 82-88
10. Lee H.S., Lee Y., Park S.S., Chae H.J. Jeon S.Y and Lee D.H. (2010), "Hydrodynamic characteristics of cold-bed circulating fluidized beds for methanol to olefins process.", *Korean J. of chemical eng.*, 27(4), 1328-1332